BPR MCS | Bulletin of Pioneering Researches of Medical and Clinical Science

Bulletin of Pioneering Researches of Medical and Clinical Science

Available online: https://bprmcs.com
2025 | Volume 5 | Issue 1 | Page: 152-163

Profiling BCL-2, iNOS, and MMP-9 Expression in Hip Synovium of Osteoarthritis Patients

Paul W. Harrison[1]*, Sara J. Bennett[1], Min Zhang[1]

[1]Department of Clinical Sciences, University of Birmingham, Birmingham, United Kingdom.

Abstract

Hip osteoarthritis (HOA) involves progressive cartilage breakdown accompanied by synovial inflammation, though the exact histopathological consequences of synovial tissue changes in HOA are not fully understood. This study investigated the expression patterns of iNOS, BCL-2, and MMP-9 within different synovial cell types. A retrospective cohort of 32 patients was analyzed, recording demographic and anthropometric data including age, sex, height, weight, and body mass index. Synovial tissue samples were examined for the presence of lymphocytes, fibrocytes, and macrophages. Clinical and histological evaluations were performed using the OARSI cartilage grading system, WOMAC index, Kellgren–Lawrence (K-L), Harris Hip Score (HHS), Krenn score and grading. Total hip arthroplasty was carried out for all patients and control subjects, with patients stratified into groups based on OA severity. Immunohistochemical staining revealed that K-L grades and Krenn scores varied significantly across the groups, including between moderate and severe OA cases. Notably, the synovial lining thickness, resident stromal cells, and inflammatory infiltrates increased in parallel with disease severity. iNOS expression in both the intimal and subintimal layers was positively associated with Krenn scores in moderate and severe OA, while BCL-2 expression in the intima correlated with Krenn score in severe OA. These findings indicate that BCL-2, iNOS, and MMP-9 contribute to synovial pathology in HOA and underscore a link between synovial inflammation, histopathological alterations, and cartilage degeneration at the time of hip replacement for OA or femoral neck fracture.

Keywords: Hip, Osteoarthritis, BCL-2, INOS, MMP-9, Cartilage

Corresponding author: Paul W. Harrison
E-mail: paul.harrison@gmail.com

Received: 18 December 2024
Revised: 09 March 2025
Accepted: 11 March 2025

How to Cite This Article: Harrison PW, Bennett SJ, Zhang M. Profiling BCL-2, iNOS, and MMP-9 Expression in Hip Synovium of Osteoarthritis Patients. Bull Pioneer Res Med Clin Sci. 2025;5(1):152-63. https://doi.org/10.51847/n7u3okhz6t

Introduction

Osteoarthritis (OA) is a progressive joint disorder that leads to deterioration of articular cartilage and adjacent joint structures, and it is a major source of pain and functional impairment in the elderly population [1–3]. Hip osteoarthritis (HOA), in particular, has a profound impact on patient quality of life and imposes significant economic burdens due to treatment costs and reduced workforce productivity [4, 5]. Symptomatic HOA affects approximately 9.2% of individuals over the age of 45 [6]. OA is a whole-joint disease, affecting not only cartilage and subchondral bone but also ligaments, menisci, and the synovial membrane, ultimately resulting in cartilage loss, synovial inflammation, subchondral sclerosis, ligament and meniscus degeneration, and osteophyte formation [1, 2]. The disease process is often initiated within the cartilage, where extracellular matrix (ECM) homeostasis is disrupted, leading to increased water content, loss of proteoglycans, and altered type II collagen synthesis [7, 8].

Inflammatory stimuli or joint trauma further enhance enzymatic activity and activate macrophages, whose degradation products stimulate chondrocytes to release proteolytic enzymes [9, 10]. Synovial macrophages ingest fragments of collagen and proteoglycans, triggering the secretion of pro-inflammatory cytokines, including interleukins (IL-1, IL-2, IL-6, IL-12), TNF-α, and cyclooxygenase-2 (COX-2) [9, 10]. These cytokines activate chondrocytes, resulting in increased matrix metalloproteinase (MMP) production and disrupted type II collagen synthesis [11]. Histopathologically, the synovial membrane in HOA exhibits thickening, increased vascularization, and infiltration by monocytes and lymphocytes [12]. The synovium comprises two layers—the intima and subintima—and contains macrophages, fibroblast-like synoviocytes (FLS), vascular endothelium, smooth muscle cells, lymphocytes, and plasma cells [13–16].

Synovial cells and chondrocytes secrete a variety of mediators, adipokines, including [14–16] cytokines, COX-2, MMPs, and inducible nitric oxide synthase (iNOS), highlighting the central role of the synovium in OA pathogenesis [17–20]. The presence of pro-inflammatory molecules in synovial fluid and histological changes in the synovial membrane support the concept that OA involves significant inflammatory components [21]. Emerging evidence suggests that FLS contribute to synovial inflammation by producing cytokines, nitric oxide (NO), and prostaglandin E2 [22]. In OA, excessive NO production by chondrocytes and synovial cells drives inflammation, inhibits ECM synthesis, promotes chondrocyte apoptosis, and contributes to pain [19, 23, 24]. MMPs, produced by both synoviocytes and chondrocytes, mediate ECM degradation by targeting collagens (types II, IX, XI) and proteoglycans, leading to irreversible joint tissue damage [25, 26].

In contrast, anti-apoptotic mechanisms, particularly through BCL-2, help maintain synovial tissue integrity by regulating mitochondrial apoptosis and preventing cytochrome c release [27]. The survival of FLS depends on a balance between anti-apoptotic signals and apoptosis, with BCL-2 overexpression conferring resistance to programmed cell death [28].

Currently, there is limited information regarding the distribution of BCL-2, iNOS, and MMP-9 in the synovial membrane of severe HOA. This study aims to investigate the relationship between the expression of these molecules in different synovial cell populations and radiological severity, histological grading, and clinical outcomes. Insights into these expression patterns could inform the development of targeted therapies for alleviating symptoms and potentially modifying disease progression in HOA.

Results and Discussion

The study included 32 patients, of whom 9 were men and 23 were women. No statistically significant differences were observed between the groups regarding age or body mass index (BMI) ($p = 0.055$ and $p = 0.884$, respectively) **(Table 1)**. The average duration of symptoms was 2.5 years for the moderate OA group and 3 years for the severe OA group. Although the Osteoarthritis Research Society International (OARSI) cartilage histopathology scores varied significantly when considering all three groups, the difference between moderate and severe OA alone was not statistically significant **(Figures 1 and 2, Table 1)**. Clinical evaluations, Similarly, Harris Hip Score (HHS), including the visual analogue scale (VAS), and McMaster Universities Osteoarthritis Index (WOMAC) and Western Ontario, did not show significant variation between the moderate and severe OA groups. In contrast, the Kellgren–Lawrence (K-L) grading system and Krenn score revealed significant differences across all groups, including a marked distinction between moderate and severe OA **(Table 1)**.

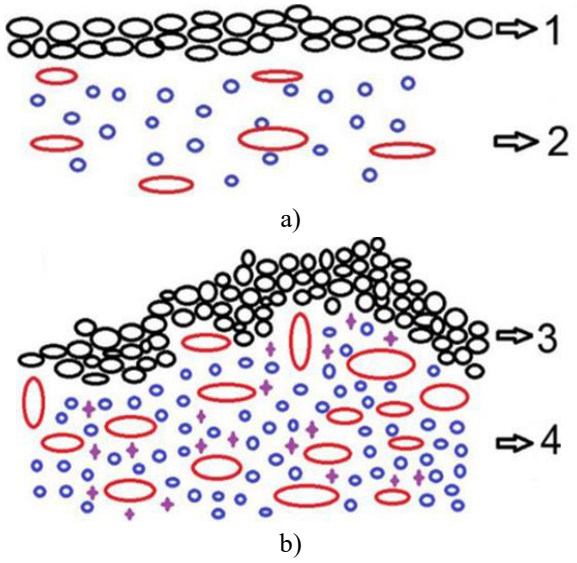

Figure 1. Illustration of the synovial membrane in patients with moderate (a) and severe (b) hip osteoarthritis (HOA). The intimal layer is depicted by black circles, and the subintimal stroma lies beneath. In moderate HOA (a), the synovial surface shows mild-to-moderate hyperplasia of synovial cells (black circles, 1), and the underlying stroma contains a moderate number of lymphocytes (blue circles, 2) along with some vascular proliferation (red circles, 2). In severe HOA (b), the synovial lining demonstrates marked papillary hyperplasia of synovial cells (black circles, 3), and the subintimal stroma exhibits dense lymphocyte infiltration (blue circles, 4), abundant macrophages (violet crosses, 4), and extensive angiogenesis (red circles, 4).

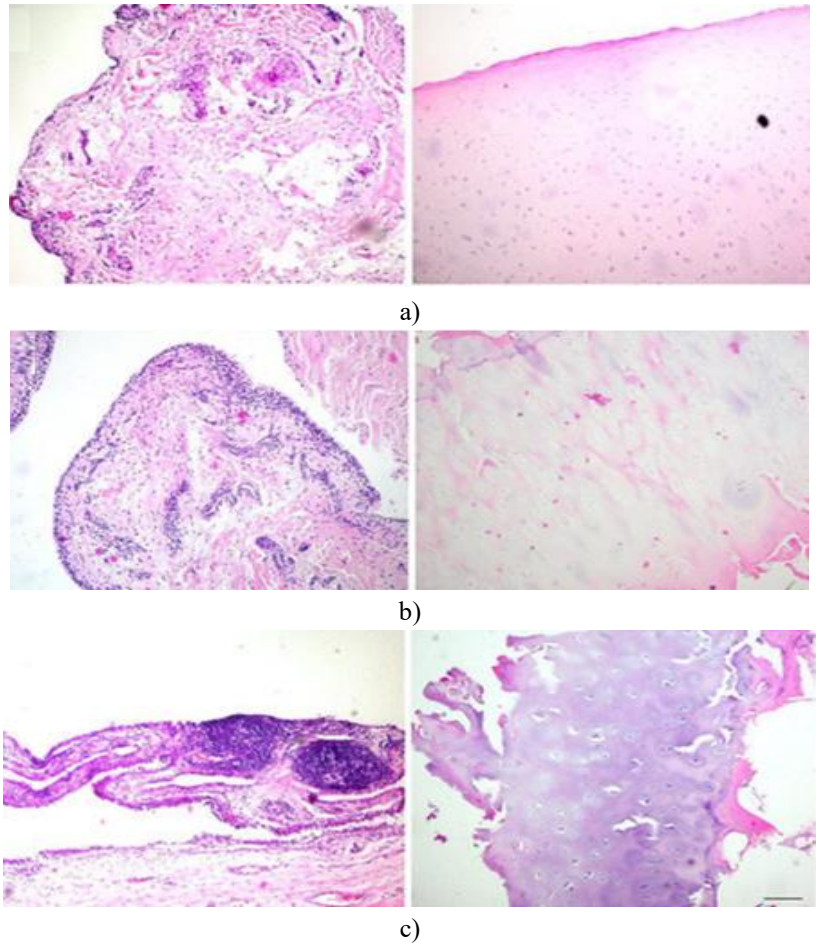

Figure 2. Histological sections of the synovial membrane (first column) and cartilage (second column) from control subjects (a) and severe (b) and hip osteoarthritis (c) patients with moderate (HOA). Samples were stained with Hematoxylin and Eosin. Images were captured at 40× magnification; scale bar = 40 µm.

Table 1. Summary of the clinical, radiological, and histopathological features of the study groups.

Characteristic	Healthy Controls (n=20)	Moderate OA (n=20)	Severe OA (n=20)	p-value
Age (years), median (IQR)	73 (72.25–76.75)	72 (63.5–75.5)	72 (67–77)	0.884
BMI (kg/m²), median (IQR)	25.67 (23.83–26.8)	24.9 (23.28–25.88)	26.9 (25.4–29.53)	0.055
Kellgren-Lawrence grade, median (IQR)	0.5 (0–1)	2 (2–2)	4 (3–4)	<0.0001
Krenn synovitis score, median (IQR)	0 (0–0)	6.5 (5.7–9)	9 (7–9)	<0.0001
OARSI cartilage score, median (IQR)	1 (0.25–1)	3 (1.5–4.5)	2.5 (2–4.7)	0.0005
Harris Hip Score (HHS), median (IQR)	–	48.9 (43.8–56.9)	41 (33.18–49.7)	0.271
VAS pain score, median (IQR)	–	6 (4.5–6.7)	6 (5–7)	0.781
Total WOMAC score, median (IQR)	–	46.1 (40–57.4)	47.3 (36.1–55.3)	0.917

VAS (visual analogue scale), OA (osteoarthritis), K-L grade (Kellgren–Lawrence grading scale), IQR (interquartile range), HHS (Harris Hip Score), BMI (body mass index), WOMAC (Western Ontario and McMaster Universities Osteoarthritis Index), OARSI (Osteoarthritis Research Society International cartilage histopathology assessment system); *p < 0.05, Kruskal–Wallace test.

Progression of OA was associated with noticeable changes in the synovium, including thickening of the lining layer, increased density of resident stromal cells, and more pronounced inflammatory infiltration. Lymphoid aggregates were absent in healthy synovial tissue, rarely observed in moderate OA, but appeared in roughly one-quarter of severe OA samples.

In the intima, iNOS expression exhibited a parabolic pattern, with the highest density observed in moderate OA (6899 ± 940.8 positive cells/mm²), and similar patterns were seen in the subintimal layer. BCL-2 levels in the intima were comparable between moderate and severe OA, yet both were elevated relative to controls. In contrast, subintimal BCL-2 showed a steady, linear increase as

disease severity advanced. MMP-9 expression within the intima rose progressively with OA severity, following a linear trend. Conversely, in the subintima, MMP-9 peaked in mild OA (3301 ± 101.6 positive cells/mm²), displaying a parabolic trend across disease stages **(Figure 3)**.

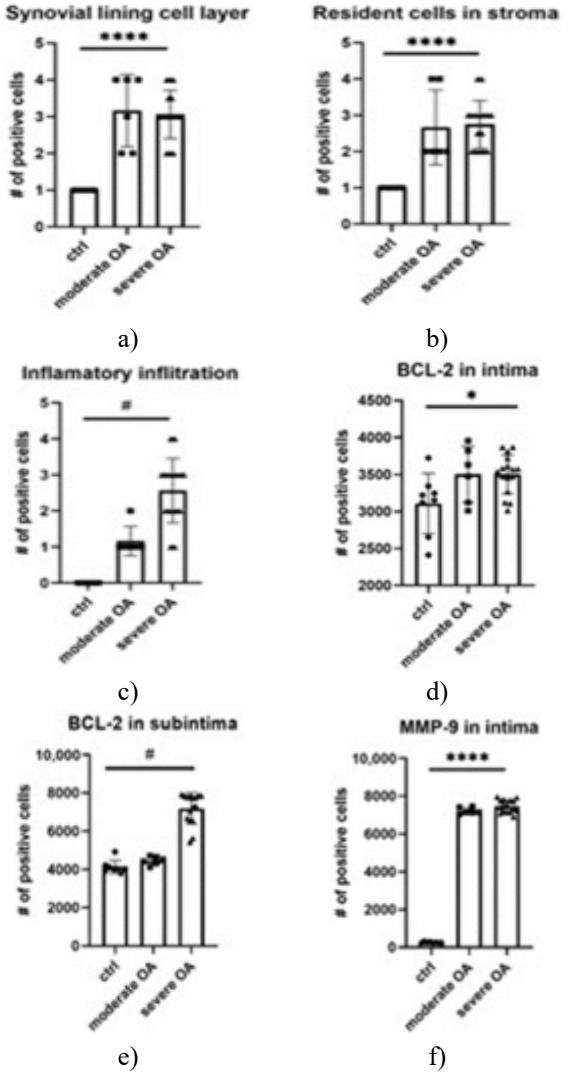

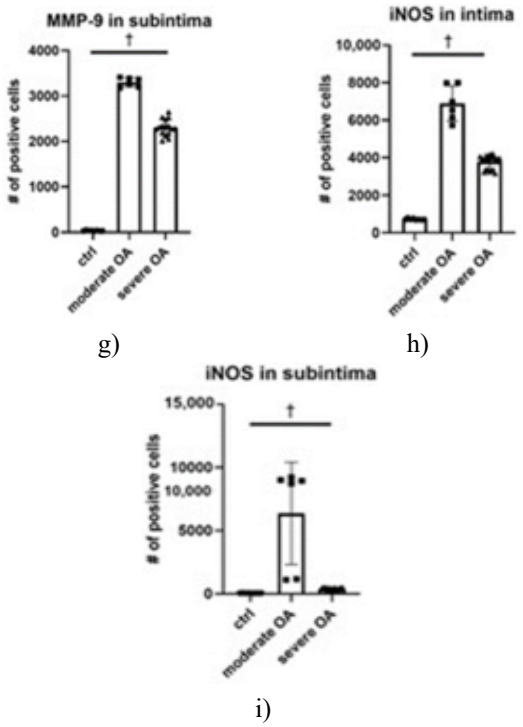

Figure 3. Overview of histopathological features and the distribution of BCL-2, MMP-9, and iNOS in the intimal and subintimal layers of patients with hip OA. Abbreviations: ctrl (control), OA (osteoarthritis); *p < 0.05, ****p < 0.0001 (ANOVA); #p < 0.05 (linear trend); †p < 0.05 (parabolic trend).

Analysis revealed that iNOS levels in both intima and subintima increased in parallel with the Krenn score in moderate and severe OA groups. In severe OA, BCL-2 expression within the intimal layer also showed a positive association with Krenn score. However, BCL-2 in the subintima, as well as MMP-9 in both layers, did not demonstrate significant correlations with Krenn scores **(Table 2)**.

Table 2. Associations between OA severity (β) and Krenn histological scores (α) with the expression of iNOS, BCL-2, and MMP-9 in intimal and subintimal compartments of OA synovium.

Immunohistochemical Marker and Synovial Layer	Control (n=20)	Moderate OA (n=20)	Severe OA (n=20)
	α | β (95% CI) | R^2	α | β (95% CI) | R^2	α (95% CI) | R^2
iNOS – Intima	0 | 727.3 (692.9–761.6) | 0%	556.6 (446.2–667)	3003 (2212–3793) | 98% *
iNOS – Subintima	0 | 59 (49.3–68.7) | 0%		7464 (7023–7904) | 99% *
BCL-2 – Intima	0 | 3110 (2769–3451) | 0%	0 | 3504 (3108–3900) | 0%	177.2 (56.26–298.1) | 2022 (1003–3041) | 41% *
BCL-2 – Subintima	0 | 4134 (3845–4423) | 0%	0 | 4460 (4230–4689) | 0%	0 | 7194 (6762–7626) | 0%
MMP-9 – Intima	0 | 261 (234–288) | 0%	0 | 7223 (7043–7404) | 0%	0 | 7465 (7292–7638) | 0%
MMP-9 – Subintima	0 | 33.88 (23.42–44.33) | 0%	0 | 3252 (2652–3852) | 0%	0 | 2184 (1304–3065) | 0%

*ANOVA p value for the model < 0.0001; α – slope; β – intercept. Values in parentheses represent the 95% confidence interval (CI) for each model parameter. The number of iNOS, BCL-2, and MMP-9 positive cells is reported as cells/mm².

Assessment of antibody staining intensity across control, moderate OA, and severe OA samples revealed that iNOS exhibited the highest signal in moderate OA, BCL-2 showed maximal staining in severe OA, and MMP-9 was

strongly expressed in both moderate and severe OA groups **(Table 3, Figures 4 and 5)**. These markers were found to co-localize with specific tissue-resident cell types, including angiogenic cells, fibroblasts, macrophages, and T-lymphocytes **(Figures 4 and 5)**.

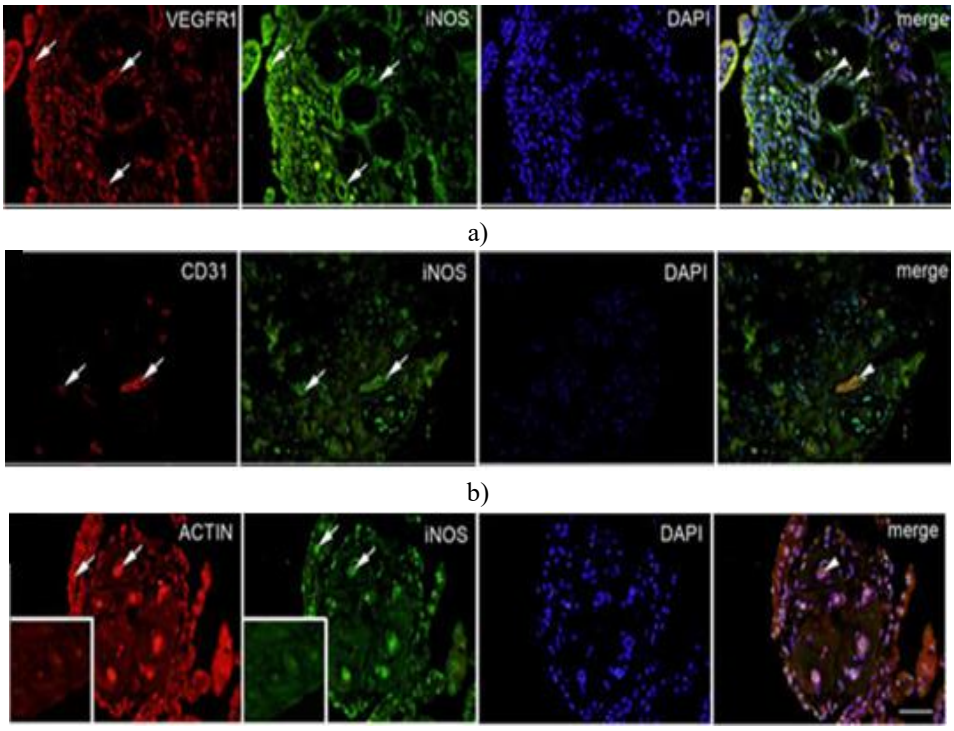

Figure 4. Immunofluorescent visualization of synovial tissue in hip osteoarthritis (HOA). (a) Moderate HOA: VEGFR1-positive cells (red) are observed within the intimal and subintimal layers (left arrow) and along vascular structures (arrows); iNOS-positive cells (green) are present in vessels and adjacent intima and subintima (arrows); nuclei are counterstained with DAPI (blue). Merged images show VEGFR1 and iNOS co-localization with nuclear staining (arrowheads, far-right panel). (b) Severe HOA: CD31-positive endothelial cells (red) highlight blood vessels (arrows); iNOS (green) localizes to both vessels and surrounding intima and subintima (arrows); DAPI (blue) labels nuclei. Merged images demonstrate overlap of CD31 and iNOS (arrowheads). (c) Severe HOA: ACTIN-positive smooth muscle cells (red) are identified in blood vessels and intima (arrows); iNOS (green) is present in vessels, intima, and surrounding subintima; nuclei are visualized with DAPI (blue). Merged panels indicate areas of co-localization of ACTIN and iNOS in vessels and intima (arrowheads). Inset shows negative control of synovial tissue. Images captured at 40× magnification; scale bar = 80 µm.

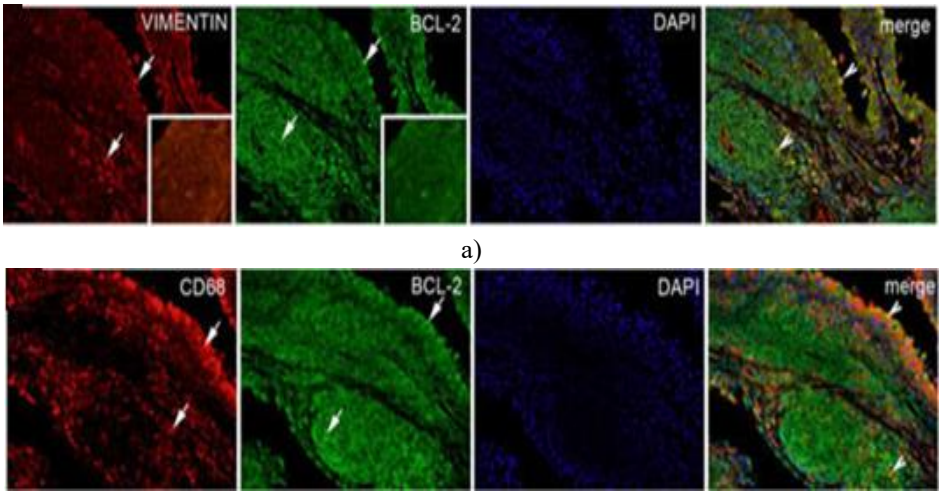

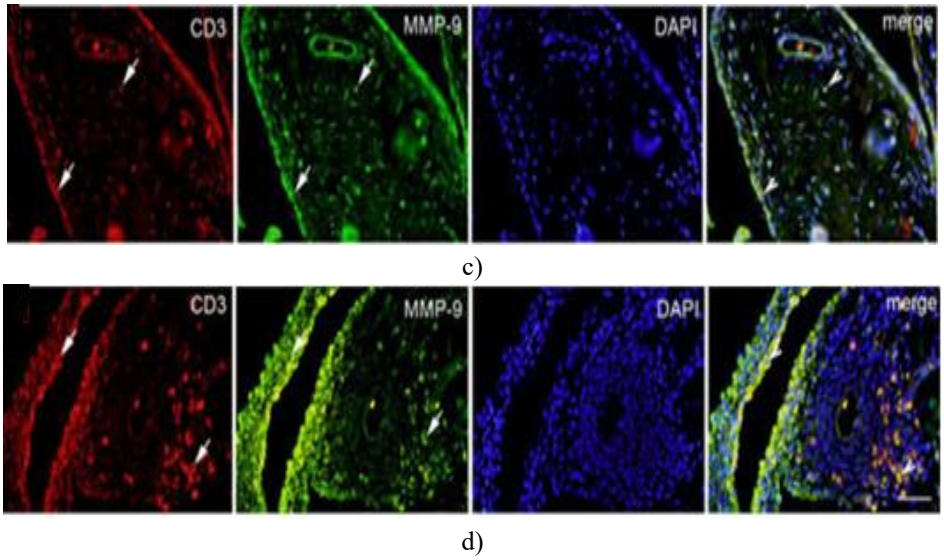

Figure 5. Immunofluorescent characterization of synovial membranes in hip osteoarthritis (HOA). (a) Severe HOA samples show Vimentin-labeled fibroblasts (red) and BCL-2-positive cells (green) distributed throughout the intimal and subintimal layers (arrows), with nuclei counterstained using DAPI (blue). The far-right merged panel demonstrates co-localization of Vimentin and BCL-2 with nuclear staining, highlighting the intima and lymph node regions (arrowheads). (b) In another set of severe HOA tissues, CD68-positive macrophages (red) co-exist with BCL-2-positive cells (green) in both synovial layers (arrows). Co-expression is visualized in the merged panel on the far-right, including the intima and lymph node (arrowheads). (c) Moderate HOA tissue displays CD3-positive lymphocytes (red) and MMP-9-positive cells (green) within intimal and subintimal compartments (arrows), with DAPI (blue) marking nuclei. The merged image shows areas of overlap between CD3 and MMP-9 (arrowheads). (d) In severe HOA, CD3 (red) and MMP-9 (green) remain co-localized across intima and subintima (arrows), and nuclear DAPI staining (blue) is present. The far-right merged panel identifies regions of CD3/MMP-9 overlap in both the intima and lymph node (arrowheads). Inset images show negative control staining of the lymph node. Magnification ×40; scale bar = 80 µm.

Table 3. Quantitative comparison of antibody staining intensity in control, moderate OA, and severe OA groups.

Antibodies	Diagnosis		
	Moderate OA	Severe OA	Control
iNOS	+++	++	+
BCL-2	++	+++	++
MMP-9	+++	+++	+

One plus indicates mild reactivity; two pluses indicate moderate reactivity; three pluses indicate strong reactivity; minus indicates no reactivity.

To evaluate angiogenic activity in the synovium, we analyzed the co-expression of iNOS, BCL-2, and MMP-9 with different angiogenesis-associated markers **(Figure 4)**. In the intima and subintima, VEGFR1+/iNOS+ cells displayed a parabolic expression pattern, peaking at 975.3 ± 10.27 and 279.3 ± 10.01 positive cells/mm², respectively, in moderate OA **(Figure 6)**. Remarkably, the subintimal VEGFR1+/iNOS+ population in moderate OA was nearly twelve times greater than in control tissues. By comparison, CD31+/iNOS+ and ACTIN+/iNOS+ populations in both synovial layers increased progressively in a linear manner as disease severity advanced, with CD31+/iNOS+ cells reaching their highest level of 75.75 ± 6.2 positive cells/mm² in severe OA.

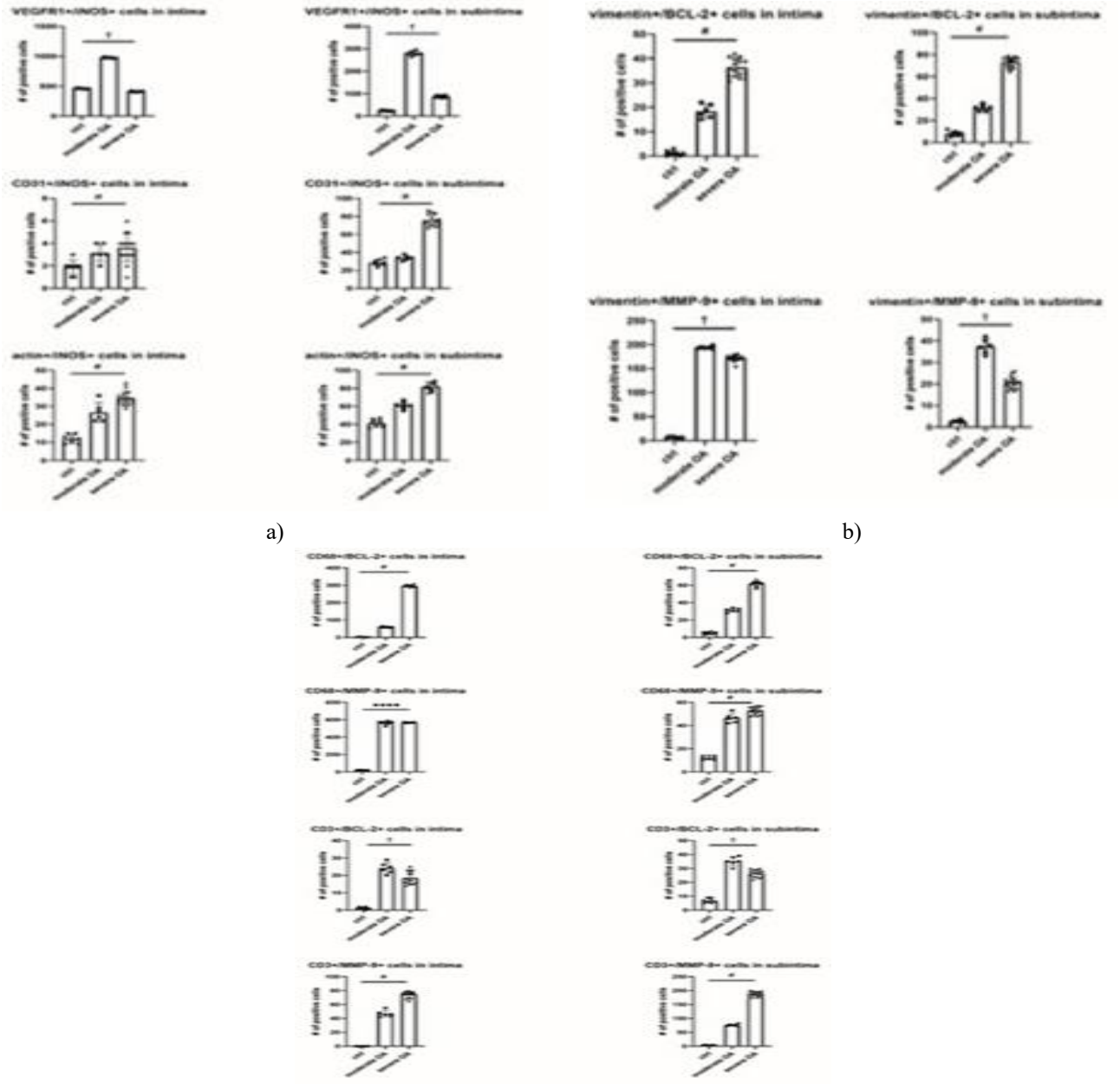

Figure 6. Distribution of VEGFR1, CD31, BCL-2, and MMP-9 in vascular cells (a), fibroblast-like cells (b), and macrophages and T cells (c) within synovial tissue from OA patients. Abbreviations: OA (osteoarthritis); ****$p < 0.0001$ for ANOVA; #$p < 0.05$ for linear trend; †$p < 0.05$ for parabolic (quadratic) trend.

To investigate the role of fibroblast-like cells in anti-apoptotic signaling and ECM remodeling, we quantified vimentin+/BCL-2+ and vimentin+/MMP-9+ populations in both intimal and subintimal layers. Vimentin+/BCL-2+ cells exhibited a linear increase with disease severity, whereas vimentin+/MMP-9+ cells followed a parabolic pattern, peaking at 194 ± 2.82 positive cells/mm² in moderate OA. In contrast, CD68+ macrophages appeared predominantly involved in anti-apoptotic processes, particularly within the intima of severe OA, and were less prominent in ECM remodeling in either layer. Regarding T-lymphocytes (CD3+), those co-expressing BCL-2 displayed a parabolic trend in the subintima, while CD3+/MMP-9+ cells increased linearly with OA progression **(Figure 6)**.

Osteoarthritis (OA) is characterized by inflammatory processes that are largely initiated by synovial macrophages. Research on knee OA has demonstrated a relationship between synovial inflammation and disease progression [29], as well as between synovial inflammation and patient-reported pain assessed using the visual analogue scale (VAS) [30]. Both synovial macrophages and fibroblast-like synoviocytes (FLS) secrete matrix metalloproteinases (MMPs) [31]. Given the significant pro-inflammatory contributions of synovial macrophages, FLS, and T cells [32] to OA pathogenesis, this study focused on their co-localization with BCL-2, MMP-9, and iNOS to better understand inflammatory alterations in the synovial membrane of patients with hip OA (HOA).

Our findings highlight ongoing inflammation, tissue remodeling, and cellular survival within the synovial membrane of HOA patients. By examining the expression of BCL-2 (anti-apoptotic marker), iNOS (pro-inflammatory and pro-angiogenic mediator), and MMP-9 (ECM degradation and angiogenesis) in the hip synovium, we aimed to correlate their levels with histopathological changes during HOA. No significant differences were observed between moderate and severe HOA groups in Harris Hip Score (HHS), WOMAC, or VAS, or in Krenn and Kellgren–Lawrence (K-L) grades. Both HHS and WOMAC scores reflect joint function, pain, and limitations in activities of daily living, which are influenced by stiffness and pain. Therefore, it is possible that the Krenn score does not directly affect joint stiffness or perceived pain. Because these scores incorporate multiple components, isolating the influence of Krenn score on specific functional outcomes is challenging, and no correlation with VAS was observed. In advanced HOA, stiffness may be driven by osteophyte formation and capsular contracture, whereas in moderate OA, reductions in HHS and WOMAC may primarily result from pain associated with synovitis.

We observed that the number of synovial lining layers, stromal resident cells, and inflammatory infiltrates increased with HOA severity, as reflected in both Krenn and K-L scores, likely due to chronic inflammation. A limitation of this study is the absence of early OA specimens, as all samples were obtained during joint replacement surgery. Previous investigations confirmed the presence of lymphoid infiltrates in OA synovia: one study on knee OA reported lymphoid aggregates in 5 of 20 synovial membranes [33], while another study examining hip and knee OA detected CD3+ aggregates in 65% of samples [34]. In our cohort, lymphoid aggregates were identified in approximately 25% of severe OA synovial membranes, consistent with the notion that these structures appear predominantly in advanced OA. Differences across studies may relate to tissue-specific influences, such as infrapatellar fat in the knee serving as a source of pro-inflammatory cytokines [35]. T cells are the main component of OA lymphoid infiltrates [36], representing roughly 22% of immune cells, while macrophages constitute the majority (~65%) of the inflamed synovial infiltrate [37]. Although prior studies focused on knee OA, our findings suggest that macrophages are similarly abundant in hip OA synovia, as indicated by the high numbers of CD68+/MMP-9+ and CD68+/BCL-2+ cells. However, relying solely on surface markers for cell identification has limitations, and these results should be interpreted cautiously. Another limitation is the observational nature of the study, which did not assess functional activity; thus, changes in marker expression may not directly reflect OA progression.

Inflammatory activity in the synovium is influenced by iNOS [38]. Ostojic *et al*. reported higher iNOS expression in early radiographic knee OA compared to advanced stages [24]. Although early OA samples were not available in our study, moderate HOA exhibited elevated iNOS levels relative to severe OA, despite lower synovitis scores. This suggests that increased iNOS expression may precede higher Krenn scores in later-stage HOA. Positive correlations between iNOS expression and Krenn score were evident across controls and HOA groups. The Krenn score is based on synovial lining thickness, stromal cellularity, and leukocyte infiltration [39].

BCL-2 expression was elevated in both moderate and severe HOA, with a linear increase in the subintima of severe OA, highlighting the importance of anti-apoptotic mechanisms in synovial inflammatory cells and FLS, which contribute to persistent inflammation. Consistent with iNOS-mediated inflammatory activity, we observed prominent co-localization of iNOS with VEGFR1-positive cells, particularly in the subintima of moderate OA patients. Vascular endothelial growth factor (VEGF), produced by inflamed synovium, may promote angiogenesis during OA [40], which can occur across all disease stages and is associated with chronic synovitis [41]. In contrast, severe OA demonstrated greater co-localization of iNOS with mature vessels, identified as CD31+ and ACTIN+ cells.

Analysis of vimentin+/MMP-9+ cells suggests that ECM remodeling is most active in moderate OA, whereas fibroblast-like cell survival, indicated by BCL-2, increases with disease progression. Elevated BCL-2 in synovial fibroblasts is well-documented in rheumatoid arthritis, contributing to inflammation [42], and appears less pronounced but similarly present in HOA, suggesting a protective effect of fibroblasts against apoptosis that may sustain synovial inflammation.

Macrophages were particularly abundant in the intima of severe OA, implying extended survival, and co-expressed MMP-9 in both HOA groups, consistent with their established role in OA pathogenesis [9]. T-lymphocytes exhibited a helper function in the subintima of moderate OA and co-expressed BCL-2 in severe OA, contributing to remodeling processes.

In conclusion, our results indicate that matrix remodeling and angiogenesis are more prominent during moderate HOA, whereas severe HOA is characterized by fibrosis, completed angiogenesis, and infiltration of long-lived macrophages.

Methods and Materials

Study population

This cross-sectional investigation was approved by the Ethics Committee of the University Hospital in Split and conducted according to the 1964 Helsinki Declaration. The study included 32 participants divided into three distinct groups: ambulatory patients older than 65 years with displaced femoral neck fractures (control group, n = 8), patients with moderate hip osteoarthritis (HOA, n = 6), and

patients with severe HOA (n = 18). Only individuals with primary HOA were eligible for the osteoarthritis groups, while those with hip dysplasia, prior hip fracture or infection, or a history of rheumatic disease were excluded.

Clinical assessment of OA patients involved the Harris Hip Score (HHS), visual analogue scale (VAS), Western Ontario and McMaster Universities Arthritis Index (WOMAC), and radiographic evaluation using the Kellgren–Lawrence (K-L) grading system. All HHS, WOMAC, and VAS measurements were performed by the same orthopedic surgeon within one month prior to surgery. For patients in the control group, HHS and WOMAC were not applicable due to their dependency on hip range of motion, and VAS was recorded exclusively for OA patients. Patients were classified as severe OA if they exhibited a K-L grade ≥ 3 and a Krenn score ≥ 7, whereas control subjects had K-L grades of 0 or 1. Standard anteroposterior hip radiographs were obtained for OA patients no more than six months before surgery.

HOA diagnosis was established in accordance with the American College of Rheumatology criteria for hip osteoarthritis classification and reporting [43]. Surgery was indicated in OA patients following unsuccessful conservative management with persistent pain and functional limitation. All participants provided written informed consent after a detailed explanation of the surgical procedure by an orthopedic surgeon. Key demographic and clinical variables, including age, sex, body mass index (BMI), duration of symptoms, and radiographic stage, were systematically documented.

Basic staining procedures and tissue collection

All patients underwent total hip replacement using the Pinnacle Acetabular Cup System and Corail Hip System (DePuy, Warsaw, IN, USA) at the Department of Orthopaedics and Traumatology, University Hospital in Split. Surgery was performed through a posterolateral approach, involving incision of the posterior capsule and detachment of the tendons of m. obturator internus, m. piriformis, and both mm. gemelli. In cases requiring luxation, the femoral neck was cut using a 1.3 mm saw (Trauma Reckon System, Synthes, Switzerland), and the femoral head with part of the femoral neck was removed. For trauma cases, hip luxation was unnecessary; the femoral head was extracted with a corkscrew following femoral neck osteotomy and partial removal of the neck.

Cartilage specimens were harvested from the weight-bearing zone of the femoral head in a triangular pattern, selecting areas adjacent to the most damaged regions but retaining some intact cartilage. Synovial tissue was collected from the inferior portion of the femoral neck, near the femoral head. Tissue collection occurred from 2017 to 2020, after which samples were fixed in formalin and transferred to the Department of Histology, Anatomy, and Embryology, University of Split School of Medicine, for histological analysis. Cartilage and subchondral bone degeneration were graded using the OARSI system, while synovial inflammation was evaluated according to the Krenn score: 0–1 for no synovitis (grade 0), 2–3 for mild synovitis (grade 1), 4–6 for moderate synovitis (grade 2), and 7–9 for severe synovitis (grade 3).

For processing, tissues were formalin-fixed, decalcified in 14% EDTA over four months, embedded in paraffin, and sectioned at 5-μm thickness. Every tenth section was stained with hematoxylin and eosin for histopathological examination.

Double immunofluorescence

For immunohistochemical evaluation, paraffin-embedded sections were first deparaffinized and gradually rehydrated through descending ethanol concentrations, following protocols described previously [44–47]. Antigen retrieval was performed by microwaving the slides in citrate buffer (pH 6.0) for 12 minutes. After allowing the slides to cool to room temperature, they were rinsed in phosphate-buffered saline (PBS) and incubated with a protein-blocking solution for 30 minutes. Sections were then exposed overnight to primary antibody mixtures as specified in **Table 4**. The following day, slides were washed with PBS and treated with the appropriate secondary antibodies **(Table 4)**. Nuclear staining was carried out using 4′,6-diamidino-2-phenylindole (DAPI), and the sections were mounted with Immu-mount and coverslipped.

Microscopy was performed using an Olympus BX51 microscope (Tokyo, Japan) equipped with a Nikon DS-Ri1 digital camera (Nikon Corporation, Tokyo, Japan). Images were captured and arranged using Adobe Photoshop (Adobe Systems, MI, USA). Ten non-overlapping fields per section were photographed at 40× magnification. Double immunofluorescence staining was conducted to detect iNOS, BCL-2, and MMP-9 together with cell-specific markers **(Table 4)**, enabling identification of positive cells in both the synovial intima and subintima. Only cells showing co-localization of both markers in either the cytoplasm or nucleus (red or green signal) were included in the counts.

Quantification of CD68+/BCL-2+, ACTIN+/iNOS+, CD31+/iNOS+, vimentin+/BCL-2+, VEGFR1+/iNOS+, CD3+/BCL-2+, vimentin+/MMP-9+, CD68+/MMP-9+, and CD3+/MMP-9+ cells was performed using ImageJ software (National Institutes of Health, Bethesda, MD, USA), expressed as the number of positive cells per mm² in both intimal and subintimal layers. For each patient, the mean value was calculated from 20 sections and compared among the control, moderate OA, and severe OA groups.

Table 4. Primary and secondary antibodies used.

Antibodies	Host	Dilution	Source	Structures Identified by Antibodies
ab59348 (polyclonal antibody)	Rabbit	1:500	Abcam (UK)	BCL-2
sc-651 (monoclonal antibody)	Rabbit	1:200	Santacruz Biotechnology (Santa Cruz, CA, USA)	iNOS
A0150 (polyclonal antibody)	Rabbit	1:100	DAKO (Gloustrup, Denmark)	MMP-9
M0823 (monoclonal antibody)	Mouse	1:20	DAKO (Gloustrup, Denmark)	CD31 (endothelial cells of blood vessels)
M0851 (monoclonal antibody)	Mouse	1:40	DAKO (Gloustrup, Denmark)	Actin (smooth muscle cells of blood vessels)
ab212369 (monoclonal antibody)	Mouse		Abcam (UK)	VEGFR1
M0725 (monoclonal antibody)	Mouse	1:50	DAKO (Gloustrup, Denmark)	Vimentin (fibroblasts)
M0876 (monoclonal antibody)	Mouse	1:75	DAKO (Gloustrup, Denmark)	CD68 (macrophages)
M7254 (monoclonal antibody)	Mouse	1:50	DAKO (Gloustrup, Denmark)	CD3 (lymphocytes)
Rhodamine Goat AP124R	Mouse	1:100	MerckMillipore (Billerica, MA, USA)	Secondary antibody
Fluorescein Goat AP132F	Rabbit	1:100	MerckMillipore (Billerica, MA, USA)	Secondary antibody

Statistical analysis

All statistical computations were carried out using GraphPad Prism (GraphPad Software, La Jolla, CA, USA). Categorical data are expressed as percentages, while ordinal and continuous measurements are presented either as medians with interquartile ranges or means with standard deviations. Group comparisons and trend evaluations were conducted using ANOVA, the Kruskal–Wallis test, and assessments for linear or quadratic (parabolic) trends. Linear regression analyses were applied to examine relationships between variables. Results are reported with R^2 values and p values, with interpretation of significance based on the recommendations of the American Statistical Association regarding p values.

Acknowledgments: None

Conflict of interest: None

Financial support: None

Ethics statement: The study was conducted according to the guidelines of the Declaration of Helsinki and approved by the Institutional Review Board (or Ethics Committee) of The Ethics Committee of the University Hospital in Split Class 500-03/17-01/75, No. 2181-147-01/06/M.S.-17-2. Issued in Split on 25 October 2017.

Informed consent was obtained from all subjects involved in the study.

References

1. Chen D, Shen J, Zhao W, Wang T, Han L, Hamilton JL, et al. Osteoarthritis: Toward a comprehensive understanding of pathological mechanism. Bone Res. 2017;5(1):16044.
2. Loeser RF, Goldring SR, Scanzello CR, Goldring MB. Osteoarthritis: A disease of the joint as an organ. Arthritis Rheum. 2012;64(6):1697–707.
3. Lawrence RC, Felson DT, Helmick CG, Arnold LM, Choi H, Deyo RA, et al. Estimates of the prevalence of arthritis and other rheumatic conditions in the United States: Part II. Arthritis Rheum. 2007;58(1):26–35.
4. Salmon J, Rat AC, Sellam J, Michel M, Eschard J, Guillemin F, et al. Economic impact of lower-limb osteoarthritis worldwide: A systematic review of cost-of-illness studies. Osteoarthritis Cartilage. 2016;24(9):1500–8.
5. Solignac M. COART France 2003 report on new socioeconomic data on osteoarthritis in France. Presse Med. 2004;33(1):4–6.
6. Jordan JM, Helmick CG, Renner JB, Luta G, Dragomir AD, Woodard J, et al. Prevalence of hip symptoms and radiographic and symptomatic hip

osteoarthritis in African Americans and Caucasians: The Johnston County Osteoarthritis Project. J Rheumatol. 2009;36(4):809–15.
7. Lahm A, Mrosek E, Spank H, Erggelet C, Kasch R, Esser J, et al. Changes in content and synthesis of collagen types and proteoglycans in osteoarthritis of the knee joint. Arch Orthop Trauma Surg. 2009;130(4):557–64.
8. Buckwalter JA, Mankin HJ, Grodzinsky AJ. Articular cartilage and osteoarthritis. Instr Course Lect. 2005;54(1):465–80.
9. Zhang H, Cai D, Bai XC. Macrophages regulate the progression of osteoarthritis. Osteoarthritis Cartilage. 2020;28(5):555–61.
10. Man GS, Mologhianu G. Osteoarthritis pathogenesis—A complex process that involves the entire joint. J Med Life. 2014;7(1):37–41.
11. Goldring MB, Otero M, Tsuchimochi K, Ijiri K, Li Y. Defining the roles of inflammatory and anabolic cytokines in cartilage metabolism. Ann Rheum Dis. 2008;67(Suppl 3):iii75–iii82.
12. de Lange-Brokaar BJ, Ioan-Facsinay A, van Osch GJ, Zuurmond AM, Schoones J, Toes RE, et al. Synovial inflammation, immune cells and their cytokines in osteoarthritis. Osteoarthritis Cartilage. 2012;20(12):1484–99.
13. Smith MD. The normal synovium. Open Rheumatol J. 2011;5(1):100–6.
14. Castrogiovanni P, Di Rosa M, Ravalli S, Castorina A, Guglielmino C, Imbesi R, et al. Moderate physical activity as a prevention method for knee osteoarthritis. Int J Mol Sci. 2019;20(3):511.
15. O'Brien K, Tailor P, Leonard C, DiFrancesco LM, Hart DA, Matyas J, et al. Enumeration and localization of mesenchymal progenitor cells and macrophages in synovium. Int J Mol Sci. 2017;18(4):774.
16. Zhang H, Lin C, Zeng C, Wang Z, Wang H, Lu J, et al. Synovial macrophage M1 polarisation exacerbates experimental osteoarthritis. Ann Rheum Dis. 2018;77(10):1524–34.
17. Sellam J, Berenbaum F. The role of synovitis in osteoarthritis. Nat Rev Rheumatol. 2010;6(11):625–35.
18. Presle N, Pottie P, Dumond H, Guillaumé C, Lapicque F, Pallu S, et al. Differential distribution of adipokines in osteoarthritis. Osteoarthritis Cartilage. 2006;14(7):690–5.
19. Abramson SB. Osteoarthritis and nitric oxide. Osteoarthritis Cartilage. 2008;16(Suppl 2):S15–S20.
20. Loeuille D, Chary-Valckenaere I, Champigneulle J, Rat AC, Toussaint F, Pinzano-Watrin A, et al. Synovial membrane inflammation in the osteoarthritic knee. Arthritis Rheum. 2005;52(11):3492–501.
21. Berenbaum F. Osteoarthritis as an inflammatory disease. Osteoarthritis Cartilage. 2013;21(1):16–21.
22. Han D, Fang Y, Tan X, Jiang H, Gong X, Wang X, et al. Fibroblast-like synoviocytes-mediated synovitis in osteoarthritis. J Cell Mol Med. 2020;24(17):9518–32.
23. Pelletier JP, Martel-Pelletier J, Abramson SB. Osteoarthritis, an inflammatory disease. Arthritis Rheum. 2001;44(6):1237–47.
24. Ostojic M, Soljic V, Vukojevic K, Dapic T. NF-κB and iNOS expression in knee osteoarthritis. J Orthop Res. 2017;35(9):1990–7.
25. Rose BJ, Kooyman DL. A tale of two joints: The role of matrix metalloproteases in cartilage biology. Dis Markers. 2016;2016(1):1–7.
26. Maldonado M, Nam J. The role of changes in extracellular matrix of cartilage in the presence of inflammation on the pathology of osteoarthritis. Biomed Res Int. 2013;2013(1):1–10.
27. Cheleschi S, Gallo I, Barbarino M, Giannotti S, Mondanelli N, Giordano A, et al. MicroRNA mediate visfatin and resistin induction of oxidative stress in human osteoarthritic synovial fibroblasts via NF-κB pathway. Int J Mol Sci. 2019;20(20):5200.
28. Hwang HS, Kim HA. Chondrocyte apoptosis in the pathogenesis of osteoarthritis. Int J Mol Sci. 2015;16(11):26035–54.
29. Ayral X, Pickering E, Woodworth T, MacKillop N, Dougados M. Synovitis as a predictive factor of structural progression of knee osteoarthritis. Osteoarthritis Cartilage. 2005;13(5):361–7.
30. Torres L, Dunlop D, Peterfy C, Guermazi A, Prasad P, Hayes K, et al. Relationship between tissue lesions and pain severity in knee osteoarthritis. Osteoarthritis Cartilage. 2006;14(10):1033–40.
31. Fuchs S, Skwara A, Bloch M, Dankbar B. Differential induction of matrix metalloproteinases in osteoarthritic synovial fibroblasts. Osteoarthritis Cartilage. 2004;12(5):409–18.
32. Li YS, Luo W, Zhu SA, Lei G. T cells in osteoarthritis: Alterations and beyond. Front Immunol. 2017;8(1):356.
33. Revell PA, Mayston V, Lalor P, Mapp P. Synovial membrane in osteoarthritis: A histological study. Ann Rheum Dis. 1988;47(4):300–7.
34. Sakkas LI, Scanzello C, Johanson N, Burkholder J, Mitra A, Salgame P, et al. T cells and cytokine transcripts in osteoarthritis synovium. Clin Diagn Lab Immunol. 1998;5(4):430–7.
35. Favero M, El-Hadi H, Belluzzi E, Granzotto M, Porzionato A, Sarasin G, et al. Infrapatellar fat pad

features in osteoarthritis. Rheumatology (Oxford). 2017;56(10):1784–93.
36. Haynes MK, Hume EL, Smith JB. Phenotypic characterization of inflammatory cells from osteoarthritic synovium. Clin Immunol. 2002;105(3):315–25.
37. Pessler F, Chen LX, Dai L, Gomez-Vaquero C, Diaz-Torné C, Paessler ME, et al. Histomorphometric analysis of synovial biopsies in joint pain disorders. Clin Rheumatol. 2008;27(9):1127–34.
38. Mapp PI, Walsh DA. Mechanisms and targets of angiogenesis and nerve growth in osteoarthritis. Nat Rev Rheumatol. 2012;8(7):390–8.
39. Krenn V, Morawietz L, Häupl T, Neidel J, Petersen I, König A. Grading of chronic synovitis. Pathol Res Pract. 2002;198(5):317–25.
40. Haywood L, McWilliams DF, Pearson CI, Gill SE, Ganesan A, Wilson D, et al. Inflammation and angiogenesis in osteoarthritis. Arthritis Rheum. 2003;48(8):2173–7.
41. Sakkas LI, Platsoucas CD. The role of T cells in osteoarthritis. Arthritis Rheum. 2007;56(2):409–24.
42. Perlman H, Georganas C, Pagliari LJ, Koch AE, Haines K, Pope RM. Bcl-2 expression in synovial fibroblasts. J Immunol. 2000;164(10):5227–35.
43. Altman R, Alarcón G, Appelrouth D, Bloch D, Borenstein D, Brandt K, et al. ACR criteria for classification of hip osteoarthritis. Arthritis Rheum. 1991;34(5):505–14.
44. Vukojevic K, Skobic H, Saraga-Babic M. Development of human spinal ganglia. Differentiation. 2009;78(2–3):91–8.
45. Juric M, Zeitler J, Vukojevic K, Bocina I, Grobe M, Kretzschmar G, et al. Connexin expression in developing human spinal cord. Int J Mol Sci. 2020;21(23):9356.
46. Kosovic I, Filipovic N, Benzon B, Bocina I, Durdov MG, Vukojevic K, et al. Connexin signaling in human kidneys. Int J Mol Sci. 2020;21(21):8349.
47. Urlic M, Urlic I, Urlic H, Masek T, Benzon B, Vitlov Uljevic M, et al. Effects of n6/n3 PUFA ratio on cardiac diabetic neuropathy. Nutrients. 2020;12(9):2761.